

# **Theoretical and experimental studies of the isomeric protonation in solution for a prototype aliphatic ring containing two nitrogens**

Peter I. Nagy,<sup>\*a,b</sup> Aditya Maheshwari,<sup>b</sup> Yong-Wah Kim<sup>c</sup> and William S. Messer, Jr.<sup>\*b,d</sup>

<sup>a</sup> Center for Drug Design and Development, The University of Toledo, Toledo, OH, 43606-3390, e-mail: [pnagy@utnet.utoledo.edu](mailto:pnagy@utnet.utoledo.edu)

<sup>b</sup> Department of Medicinal and Biological Chemistry, The University of Toledo

<sup>c</sup> Department of Chemistry, The University of Toledo

<sup>d</sup> Department of Pharmacology, The University of Toledo, Toledo, OH, 43606-3390, e-mail: [wmesser@utnet.utoledo.edu](mailto:wmesser@utnet.utoledo.edu)

## **Supporting Information**

## Contents

Experimental section

Monte Carlo simulations

Table S1. Protonated N-methyl piperidine atomic charges for Monte Carlo simulations.

Calculation of the tautomeric ratio on the basis of NMR spectra

Table S2. Chemical shifts in different solvents at different concentrations.

Table S3. Calculated proton affinities and gas-phase basicities for piperidine, N-methyl piperidine and piperazine.

Table S4a. IEF-PCM internal energies for protonated N-Me piperazine species in solution.

Table S4b. IEF-PCM solvation free energies for protonated N-Me piperazine species

Fig. S1. Compound 4:  $^1\text{H}$  NMR in  $\text{CDCl}_3$ , ambient temperature

Fig. S2. Compound 5:  $^1\text{H}$  NMR in  $\text{CD}_2\text{Cl}_2$ , ambient temperature

Fig. S3. Compound 5: COSY in  $\text{CD}_2\text{Cl}_2$ , ambient temperature

Fig. S4. Compound 1:  $^1\text{H}$  NMR (1 mg/1.5 ml  $\text{D}_2\text{O}$ ), ambient temperature

Fig. S5. Compound 1:  $^1\text{H}$  NMR (75 mg/1.5 ml  $\text{D}_2\text{O}$ ), ambient temperature

Fig. S6. Compound 2a/b:  $^1\text{H}$  NMR (75 mg/1.5 ml  $\text{D}_2\text{O}$ ), ambient temperature

Fig. S7. Compound 3:  $^1\text{H}$  NMR (1 mg/1.5 ml  $\text{D}_2\text{O}$ ), ambient temperature

Fig. S8. Compound 3:  $^1\text{H}$  NMR (75 mg/1.5 ml  $\text{D}_2\text{O}$ ), ambient temperature

Fig. S9. Compound 1:  $^1\text{H}$  NMR (75 mg/1.5 ml  $\text{CD}_2\text{Cl}_2$ ), ambient temperature

Fig. S10. Compound 2a/b:  $^1\text{H}$  NMR (75 mg/1.5 ml  $\text{CD}_2\text{Cl}_2$ ), ambient temperature

Fig. S11. Compound 2a/b:  $^1\text{H}$  NMR (75 mg/1.5 ml  $\text{CD}_2\text{Cl}_2$ ), 166 K

Fig. S12. Compound 2a/b: COSY (75 mg/1.5 ml  $\text{CD}_2\text{Cl}_2$ ), 166 K

Fig. S13. The (NMpt.HCl) dimer in DCM

Fig. S14. The (NMpt.HCl) dimer in water

Fig. S15. Water- protonated N-methyl piperazine pair-energy distribution functions for NMpt and NMps solutes.

Fig. S16. Solute-solvent pair-energy distribution functions for NMpt and NMps solutes in acetonitrile and dichloromethane solvents

## *Experimental Section*

### Organic syntheses

Experiment 1: N-methyl piperazine (0.7 ml, 6.31 mmol) was dissolved in diethyl ether (25 ml) and 1N HCl (6.31 ml, 6.31 mmol) was added slowly at room temperature. The reaction mixture was stirred for 1 h. The solvent was removed under vacuum. Water and traces of HCl were removed using lyophilization. The resulting compound was dissolved in anhy. dichloromethane (25 ml), filtered and concentrated to give compound **2a/b** (732 mg, 84.9 %) as yellowish-brown solid. The white solid retained on filtered paper was washed with dichloromethane (3 x 1 ml) and dried to yield compound **3** (41 mg, slight crude) as a minor product.

Experiment 2: N-methyl piperazine (0.7 ml, 6.31 mmol) was dissolved in diethyl ether (25 ml) and 1N HCl in diethyl ether (6.31 ml, 6.31 mmol) was added slowly at room temperature. The reaction mixture was stirred for 1 h. The solvent was removed under vacuum. The resulting compound was dissolved in anhy. dichloromethane (25 ml), filtered and concentrated to give compound **2a/b** (758 mg, 87.9 %) as yellowish-brown solid. The white solid retained on filtered paper was washed with dichloromethane (3 x 1 ml) and dried to yield compound **3** (35 mg) as a minor product.

Compound **2a**;  $^1\text{H NMR}$  ( $\text{CD}_2\text{Cl}_2$ , ambient temperature); 9.5 (1 H, s), 3.2-3.14 (4 H, t,  $J = 5.4$  Hz), 2.68-2.62 (4 H, t,  $J = 5.4$  Hz), 2.3 (3 H, s).

Compound **2a**;  $^1\text{H NMR}$  ( $\text{CD}_2\text{Cl}_2$ ,  $-107^\circ\text{C}$ ); 9.62 (1 H, s), 9.31 (1 H, s), 3.4-3.2 (2 H, m), 3.1-2.6 (4 H, m), 2.4-1.9 (5 H, m).

Compound **3**;  $^1\text{H NMR}$  ( $\text{D}_2\text{O}$ , ambient temperature); 3.9-3.1 (8 H, s), 2.84 (3 H, s).

Compound **4**;  $^1\text{H NMR}$  ( $\text{CDCl}_3$ , ambient temperature); 3.0-2.9 (2H, m), 2.6-2.5 (2H, m), 1.62-1.54 (2H, m), 1.48-1.34 (1H, m), 1.1-0.98 (2H, m), 0.9-0.86 (3H, d,  $J = 6.8$  Hz).

Compound **5**;  $^1\text{H}$  NMR ( $\text{CD}_2\text{Cl}_2$ , ambient temperature); 11.7 (1 H, s), 3.6-2.4 (7 H, m), 2.2-1.1 (6 H, m).

### NMR

All the commercially available reagents and solvents were used without purification. NMR spectra were obtained using 600 MHz and 400 MHz instruments. In  $^1\text{H}$  NMR, chemical shifts were referenced and expressed in ppm relative to the central peak of deuterium oxide (4.63 ppm), deuterated methylene chloride (5.32 ppm) and chloroform-d (7.26 ppm) (Figs. S1-S12). NMR samples (deuterated methylene chloride & chloroform-d) were dried overnight over molecular sieves before running NMR experiments. Since the water peaks are affected by concentration and samples, all  $^1\text{H}$  NMR data were referenced externally also to TSP in  $\text{D}_2\text{O}$ .

### *Monte Carlo Simulations*

Monte Carlo simulations were performed at  $T=298$  K and  $p=1$  atm in NpT (isobaric-isothermal) ensembles<sup>23</sup> for calculating relative solvation free energies for the tautomeric protonation of N-methyl piperazine in water, acetonitrile and dichloromethane (DCM) solvents. Using the BOSS 4.7 program,<sup>24</sup> solution models were established by considering a cation with and without a chloride anion in solvent boxes. Solvent boxes were comprised of 504 TIP4P-water,<sup>25</sup> 264 acetonitrile, and 264 DCM molecules. Three point models of Jorgensen et al. for acetonitrile<sup>26a</sup> and DCM<sup>26b</sup> were utilized. The interaction energy of the solution elements was calculated by using the all-atom 12-6-1 OPLS-AA pair potential.<sup>27</sup> 12-6 OPLS parameters were taken from the program library. The atomic charge parameters were obtained by a fit to the in-solution IEF-PCM/B3LYP/6-31G\* molecular electrostatic potential (ELPO) using the CHELPG<sup>28</sup> and RESP<sup>29</sup> fitting procedures. In predicting solvent effects, charges fitted to the 6-31G\* ELPO proved superior to charges fitted to the 6-311++G\*\* ELPO.<sup>11,12a</sup> Periodic boundary conditions and preferential sampling proportional to a weight factor of  $1/(R^2 + 120)$  were applied, where  $R$  is the distance of the reference solute atom and the reference atom of the selected solvent molecule. Other simulation parameters were close to those used in recent calculations.<sup>11,12</sup>

Table S1. Atomic charges applied in Monte Carlo simulations in different solvents. The values were derived by a fit to the in-solution IEF-PCM/B3LYP/6-31G\* molecular electrostatic potential

	dichloromethane	acetonitrile	water	
	CHELPG	CHELPG	CHELPG	RESP
N-methyl piperazine				
$H^+N(t)$				
$N_1(t)$	0.1910	0.2019	0.2073	-0.0165
$C_2$	-0.2057	-0.2084	-0.2109	-0.1587
$H(C_2)$ eq,ax	0.1145, 0.1558	0.1158, 0.1559	0.1165, 0.1557	0.1298, 0.1661
$C_3$	0.2379	0.2371	0.2378	0.0229
$H(C_3)$ eq,ax	0.0736, 0.0076	0.0715, 0.0104	0.0711, 0.0108	0.0784, 0.0610
$N_4(s)$	-0.7836	-0.7911	-0.7930	-0.6730
$H_{eq}N_4$	0.3907	0.3906	0.3913	0.3883
$H_{ax}N_1$	0.2846	0.2875	0.2872	0.3344
$C_{met}$	-0.3434	-0.3479	-0.3503	0.0610
$H_{met}$ sp,osp <sup>a</sup>	0.1661, 0.1636	0.1658, 0.1643	0.1663, 0.1646	0.0636, 0.0614
$H^+N(s)$				
$N_1(t)$	-0.3938	-0.3976	-0.3971	-0.3761
$C_2$	0.0555	0.0550	0.0525	-0.0794
$H(C_2)$ eq,ax	0.1150, 0.0636	0.1136, 0.0662	0.1135, 0.0672	0.1437, 0.0981
$C_3$	-0.1295	-0.1318	-0.1332	-0.0777
$H(C_3)$ eq,ax	0.1140, 0.1415	0.1153, 0.1408	0.1163, 0.1409	0.1095, 0.1323
$N_4(s)$	-0.0864	-0.0798	-0.0800	-0.0639
$H_{eq}N_4$	0.3097	0.3110	0.3136	0.2986
$H_{ax}N_4$	0.3128	0.3145	0.3169	0.3130
$C_{met}$	-0.1383	-0.1390	-0.1380	0.0500
$H_{met}$ sp,osp <sup>a</sup>	0.0671, 0.1043	0.0667, 0.1030	0.0666, 0.1018	0.0516, 0.0222

The molecules have  $C_s$  symmetry, making  $C_2$  and  $C_6$ , as well as  $C_3$  and  $C_5$  atoms and the corresponding bound hydrogen atoms bearing equal charges. <sup>a</sup>The sp and osp hydrogen atoms are located in the symmetry plane (sp) and out-of-symmetry plane (osp).

The FEP method<sup>21</sup> was applied along nonphysical perturbation paths, by developing and annihilating hydrogen atoms at the required sites for the six-member rings with two nitrogen atoms. Since the free energy is a state function, the final result is independent of the perturbation path, which can be even a nonphysical route. The interaction potential and geometry parameters were calculated as a linear function of the reference parameters defined at the two end-points of the perturbation route. Using double-wide sampling, the perturbation step parameter was chosen so that the free energy increments did not exceed about 1 kcal/mol.  $7.5 \times 10^6$  (7.5M) configurations were considered both in the equilibration and averaging phases at every step.

The pmf curves were calculated for both tautomers. Considering 2 moles of ion-pairs in boxes of 496 TIP4P water and 257 DCM molecules and applying Ewald summation, the pmf's were calculated by increasing the distance of the ring centers,  $R_c$  by 0.2 Å steps in the 4.5-12.0 Å range, and  $\Delta G$  was calculated at  $R_c \pm 0.1$  Å. Equilibration of the systems was allowed by considering 15 M configurations and averaging was taken over another 7.5 M configurations at every pmf step. The separation of the ring centers was kept constant at  $R_c$ , thus the rings could translate only in tandem, but the rings could rotate independently around randomly selected axes through the ring centers. No restriction was imposed on the move of the anions. A move for a randomly selected solute was attempted every 25 steps.

### *Calculation of the tautomeric ratio on the basis of NMR spectra*

$^{14}\text{N}$  is 99.64% abundant and has a relatively large quadrupole moment. Broadening of the proton resonance, which results from faster relaxation time due to scalar coupling to the  $^{14}\text{N}$ , is a problem in DNMR studies.<sup>33a</sup> A doublet for methyl protons was not observed because the relaxation time for N-H protons is less than  $1/J$ . Omitting relaxation effects, the gs-COSY cross peak intensity is given by<sup>33b</sup>

$$\sin(\Omega_1 t_1) \sin(\pi J t_1) \sin(\Omega_2 t_2) \sin(\pi J t_2) \quad (14)$$

where  $\Omega_1$  and  $\Omega_2$  are the chemical shifts of N-H and methyl protons, respectively, and  $J$  is the coupling between the protons.  $t_1$  and  $t_2$  are the evolution time in the 1<sup>st</sup> and 2<sup>nd</sup> dimension, respectively. Provided  $t_1$  is not too short, it can be shorter than  $1/J$  and yet the above term can still give rise to an observable gs-COSY cross peak.

The N(t) : N(s) ratio for the dissolved monosalt in  $\text{D}_2\text{O}$  was calculated at about 20:80. In principle, this ratio could be confirmed by measuring the intensity of N(t) proton and N(s) proton in the  $^1\text{H}$  NMR spectrum. However, the  $^1\text{H}$  NMR spectrum of the monosalt in  $\text{D}_2\text{O}$  contains only 4 distinct peaks (Figure S7). With distinct N(t) and N(s) species, more than twice that number of peaks are expected. Rapid intermolecular proton exchange is responsible for the coalescence of NMR lines resulting in only 4 broadened lines.

There are two sets of peaks at 3.24ppm and 2.84ppm for the  $\text{CH}_2$  protons and one at 2.45ppm for the methyl protons. There is only one peak at 4.86ppm for water protons and the N-H protons associated with N(t) and N(s) due to rapid proton exchange between the molecules. The water hydrogen, H is associated with mostly  $\text{H}_2\text{O}$  and small amounts of  $\text{H}_3\text{O}^+$  and  $\text{HO}^-$  species. The exchange rate cannot be slowed down sufficiently by cooling the sample because water freezes before the colder temperatures can be reached.

In the fast exchange limit, the chemical shift of the coalesced NMR line is the weighted average of the chemical shifts of the individual chemical shifts<sup>33c</sup>.

For the two-step protonation of N-methyl-piperazine,  $\text{pK}_{a1} = 9.20$  and  $\text{pK}_{a2} = 5.07$ . Therefore in the aqueous solution of the monosalt, the  $\text{CH}_3$  protons can be part of 3 molecular species: free base, the protonated N(s) and the protonated N(t) species. In monosalt solutions of 75mg/1.5ml concentration, about 0.0042% of the monosalt



molecules would dissociate to give the free base molecule. Therefore the contribution from the free base molecular species to the measured chemical shift of CH<sub>3</sub> proton is negligible and can be dropped. Using a two-site exchange model where the molecule exchanges rapidly between the singly-protonated N(s) and N(t) species shifts<sup>33</sup>. The chemical shift of the CH<sub>3</sub> protons in a solution of mono-protonated salt is as follows:

$$\delta = P_s\delta_s + P_t\delta_t \quad \text{and} \quad P_s + P_t = 1 \quad (1a,b)$$

where P<sub>s</sub> and P<sub>t</sub> are the probabilities of the N(s) and N(t) species, respectively.

To estimate the ratio P<sub>t</sub> : P<sub>s</sub>, we need to know δ<sub>t</sub> and δ<sub>s</sub>, the chemical shifts of CH<sub>3</sub> protons for the pure N(t) and N(s) species, respectively. First, we will need to determine the amount of chemical shifts that will arise from structural changes from a free base molecule to the mono- protonated N(s) and N(t) species in D<sub>2</sub>O.

Table. S2. Chemical shifts in different solvents at different concentrations. Structure codes in the first column. Probability values were calculated on the basis of 75mg/1.5ml data.

---

	NMR solvent	Concentration	δCH <sub>3</sub>
<b>1</b>	D <sub>2</sub> O	1 mg/1.5 ml	2.2339
<b>1</b>	D <sub>2</sub> O	75 mg/1.5 ml	2.2130
<b>1</b>	CD <sub>2</sub> Cl <sub>2</sub>	75 mg/1.5 ml	2.1809
<b>2a/2b</b>	D <sub>2</sub> O	75 mg/1.5 ml	2.4459
<b>2a/2b</b>	CD <sub>2</sub> Cl <sub>2</sub>	75 mg/1.5 ml	2.2978
<b>3</b>	D <sub>2</sub> O	75 mg/1.5 ml	3.0246
<b>3</b>	D <sub>2</sub> O	1 mg/1.5 ml	2.9643

---

The impact of structural changes on the chemical shift was explored in dichloromethane solution, where we could lower the temperature substantially. In DCM at room temperature, there were still 4 peaks observed for the solution of the monosalt. Due to hydrogen bonding, the chemical shift of N-H protons is 9.50ppm, a value remarkably higher than the usual chemical shift of amine protons around 2.4 to 3.2ppm.

For the structural reasons, see Fig. 2 in the paper. COSY experiments in DCM at  $-107^{\circ}\text{C}$  (166 K), confirmed that the solute molecule adopts the N(s)-protonated form. In DCM at room temperatures, the chemical shift for the methyl proton in case of the N(s) monosalt is higher than that of the free base by 0.1169ppm.

Since the NMR solvent used will affect the observed chemical shifts, the chemical shifts from samples dissolved in  $\text{D}_2\text{O}$  is used. The chemical shift of the methyl proton in N(s),  $\delta_s$ , can be calculated using the chemical shift for the free base molecule in  $\text{D}_2\text{O}$ , and applying a correction due to structural changes associated with picking up an extra proton at the N(s) site. Since the free base is basic, some fraction of these molecules will pick up an extra proton. However, in a more concentrated sample the population of mono-protonated molecule can be minimized. Using  $\text{pK}_{\text{a}1} = 9.20$  and a concentration of 75mg/1.5ml, the protonated fraction of the free base molecule is only 0.56%. Thus, considering the chemical shift of methyl protons for the free base and the empirical correction term obtained on the basis of the DCM experiment, the chemical shift of molecule with N(s) protonation was estimated as  $\delta_s = 2.330\text{ppm}$ . Using the estimated dissociation of both the dilute and concentrated solutions of free base, a linear extrapolation to a solution where none of the free base molecules acquire an extra proton, the value of  $\delta_s = 2.327\text{ ppm}$  was obtained. This is 0.0028ppm smaller than that calculated above.

The chemical shift of the molecule with N(t) protonation,  $\delta_t$  can be obtained from a more concentrated solution of disalt in  $\text{D}_2\text{O}$ . 0.53% dissociation of disalt is predicted for a concentration of 75mg/1.5ml. Starting with the chemical shift of the methyl proton from the doubly protonated molecule, the removal of a proton from the N(s) site would move the chemical shift of CH3 protons down giving a chemical shift of  $\delta_t = 2.908\text{ppm}$ . Using the estimated dissociation of both the dilute and concentrated solutions of disalt, and extrapolating linearly to a solution with no dissociation,  $\delta_t = 2.916\text{ ppm}$ . This 0.0081ppm larger than that calculated above.

Accepting the empirically predicted chemical shifts, eqs. 1a and 1b can be solved to give the ratio of the populations of N(t):N(s) to be 20.1:79.9 Using the chemical shifts  $\delta_s$  and  $\delta_t$  obtained by extrapolating to 100% free base and 100% disalt, the population ratio of N(t):N(s) was calculated at 20.3:79.7. Thus ignoring the 0.53% dissociation of disalt

and 0.56% protonation of free base will result in an underestimation of the population of N(t) by 1%.

The N(t):N(s) ratio of about 20:80 obtained by the NMR experiments is in good agreement with the ratio of 22:78 estimated on the basis of our theoretical model.

Table S3. Calculated energy, enthalpy (proton affinity) and free energy (basicity) changes for the reaction  $\text{BH}^+ \leftrightarrow \text{B} + \text{H}^+$  in the gas phase at  $T = 298 \text{ K}$  and  $p = 1 \text{ atm}^a$

	$\Delta E$	$\Delta H(T)^b$	$T\Delta S(T)^c$	$\Delta G(T)$	$\Delta H_{\text{exp}}^d$	$\Delta G_{\text{exp}}$
B3LYP/6-31G*						
Piperidine	239.5	231.2	7.6	223.6		
N-Me piperidine	242.2	233.8	7.5	226.3		
Piperazine <sup>e</sup>	238.4	230.4	7.1	223.2		
B3LYP/6-311++G**						
Piperidine	236.3	228.0	7.6	220.4	228.0	220.1
N-Me piperidine	240.0	231.5	7.6	224.0	232.1	224.7
Piperazine <sup>e</sup>	234.9	226.8	7.2	219.7	225.6	218.6
B3LYP/aug-cc-pvtz//B3LYP/6-311++G**						
Piperidine	236.4					
N-Me piperidine	240.1					
Piperazine	235.0					
	$\Delta E$					
	MP2 aug-cc-pvdz	MP2 aug-cc-pvtz/SP	MP2 <sub>CBS</sub>	QCISD(T) aug-cc-pvdz/SP	QCISD(T) <sup>f</sup> CBS	
Piperidine	234.1	234.5	234.7	235.7	236.3	
N-Me piperidine	238.2	238.5	238.7	240.1	240.5	
Piperazine	232.5	233.0	233.2	234.2	234.9	

<sup>a</sup>Energies in kcal/mol. <sup>b</sup> $5/2 RT = 1.48 \text{ kcal/mol}$  for the proton kinetic energy and the volume work is included (See also Ref. 6b). <sup>c</sup>The TS product for the proton was assumed as  $7.76 \text{ kcal/mol}$  (Refs. 6b, 12). <sup>d</sup>The experimental values (Ref. 19) provided in  $\text{kJ/mol}$  were converted to  $\text{kcal/mol}$  as  $4.184 \text{ kJ/mol} = 1 \text{ kcal/mol}$ . No uncertainty was provided for the experimental values. <sup>e</sup>A rotational symmetry number of 2 was considered for calculating the entropy of the unprotonated piperazine with  $C_{2h}$  symmetry. <sup>f</sup>The  $\Delta E$  values were calculated as  $\Delta E(\text{QCISD(T)/CBS}) = \Delta E(\text{MP2}_{\text{CBS}}) + (\Delta E(\text{QCISDT(aug-cc-pvdz)}) - \Delta E(\text{MP2(aug-cc-pvdz)}))$ . The  $\Delta E(\text{MP2}_{\text{CBS}})$  values were estimated on the basis of aug-cc-pvdz optimization and aug-cc-pvtz single-point calculations. MP2 thermal corrections deviate from the B3LYP/6-311++G\*\* values by  $\pm 0.1 \text{ kcal/mol}$ .

Table S4a. IEF-PCM internal energies in solution for protonated N-Me piperazine species relative to the tautomer in chair conformation and protonated at the tertiary nitrogen<sup>a</sup>

	B3LYP 6-31G*	B3LYP 6-311++G**/SP	B3LYP cc-pvtz/SP	B3LYP aug-cc-pvtz/SP	B3LYP 6-311++G**
Water	3.89	4.58	4.52	4.60	4.63
TB(t) <sup>b</sup>	3.36	3.49			
TB(s) <sup>b</sup>	7.43	8.06			
CH <sub>3</sub> CN	3.77	4.45	4.39	4.47	4.56
CH <sub>2</sub> Cl <sub>2</sub>	3.71	4.40	4.31	4.40	4.42
H <sub>eq</sub> <sup>+</sup> ..Cl <sup>-c</sup>	3.08	3.46			
H <sub>ax</sub> <sup>+</sup> ..Cl <sup>-c</sup>	2.11	2.74			
TB(t) <sup>d</sup>	3.58	3.81			
TB(s) <sup>d</sup>	7.31	8.04			
	QCISD(T) 6-31G*/SP	QCISD(T) cc-pvtz/SP	MP2 <sub>CBS</sub>	QCISD(T)/CBS <sup>e</sup>	MP2 6-31G*
Water	4.14	5.03	4.84	5.01	
CH <sub>3</sub> CN	4.04	4.95	4.82	4.99	
CH <sub>2</sub> Cl <sub>2</sub>	4.01	4.88	4.66	4.83	
H <sub>eq</sub> <sup>+</sup> ..Cl <sup>-c</sup>					5.13
H <sub>ax</sub> <sup>+</sup> ..Cl <sup>-c</sup>					3.21

<sup>a</sup>Energies in kcal/mol. Unless indicated, energy values are provided for the tautomer protonated at the secondary nitrogen. Single-point (SP) calculations were performed at the B3LYP/6-31G\* optimized geometry. <sup>b</sup>Twist-boat conformations with protonation at the (t)ertiary and the (s)ecundary nitrogen. <sup>c</sup>A chloride anion in a hydrogen bond with the protonating atom. Subscripts indicate the equatorial or axial position of the involved hydrogen. Reference structure is a chair, N-Me piperazine, protonated at the tertiary nitrogen and a chloride is in hydrogen bond with the N-H bond. <sup>e</sup>MP2<sub>CBS</sub> and post-MP2 corrections (eq. 7) were calculated at the MP2/aug-cc-pvdz optimized geometries.

Table 4b. IEF-PCM solvation free energies for protonated N-Me piperazine species relative to the tautomer in chair conformation and protonated at the tertiary nitrogen<sup>a</sup>

	B3LYP 6-31G*	B3LYP 6-311++G**/SP	B3LYP cc-pvtz/SP	B3LYP aug-cc-pvtz/SP	B3LYP 6-311++G**
Water	-4.56	-4.48	-4.64	-4.54	-4.52
TB(t) <sup>b</sup>	2.28	2.57			
TB(s) <sup>b</sup>	-2.40	-2.02			
CH <sub>3</sub> CN	-4.23	-4.15	-4.32	-4.21	-4.25
CH <sub>2</sub> Cl <sub>2</sub>	-3.79	-3.72	-3.83	-3.75	-3.74
H <sub>eq</sub> <sup>+</sup> ..Cl <sup>-c</sup>	-3.36	-3.22			
H <sub>ax</sub> <sup>+</sup> ..Cl <sup>-c</sup>	-1.77	-1.68			
TB(t) <sup>d</sup>	1.63	1.80			
TB(s) <sup>d</sup>	-2.09	-1.82			
	HF 6-31G*/SP		HF cc-pvtz/SP	HF aug-cc-pvtz	HF 6-31G*
Water	-4.33		-4.51	-4.50	
CH <sub>3</sub> CN	-4.01		-4.18	-4.30	
CH <sub>2</sub> Cl <sub>2</sub>	-3.62		-3.74	-3.72	
H <sub>eq</sub> <sup>+</sup> ..Cl <sup>-c</sup>					-4.35
H <sub>ax</sub> <sup>+</sup> ..Cl <sup>-c</sup>					-2.06

<sup>a</sup>Energies in kcal/mol. For the explanation of the superscripts, see Table S4a. For /SP calculations the B3LYP/6-31G\* optimized geometries were accepted. The HF/aug-cc-pvtz and HF/6-31G\* solvation free energies were calculated at geometries optimized at the MP2/aug-cc-pvdz and MP2/6-31G\* level, respectively.

NMR spectra

Compound 4:  $^1\text{H}$  NMR in  $\text{CDCl}_3$ , ambient temperature

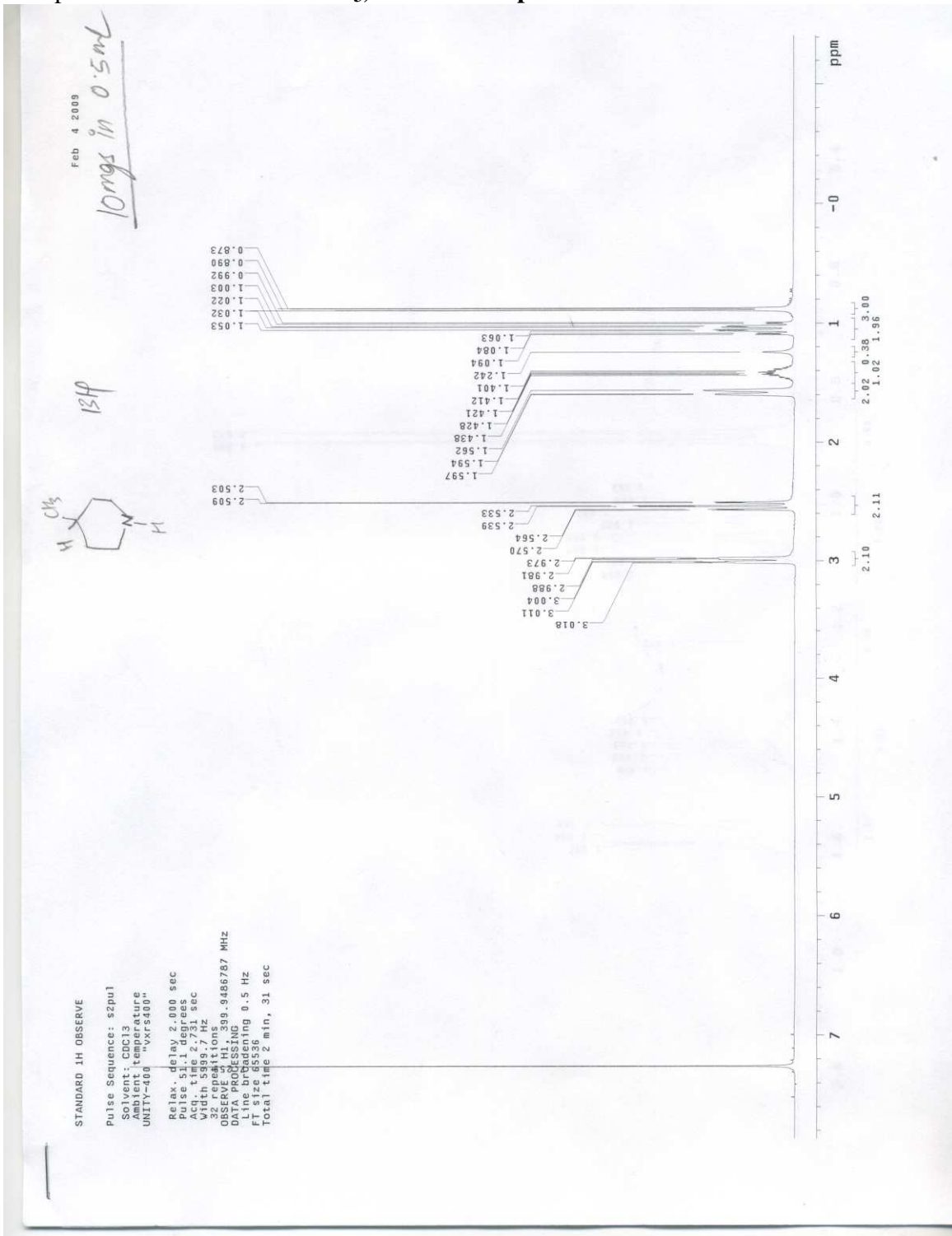


Fig. S1.







Compound 1:  $^1\text{H}$  NMR (1 mg/1.5 ml  $\text{D}_2\text{O}$ ), ambient temperature

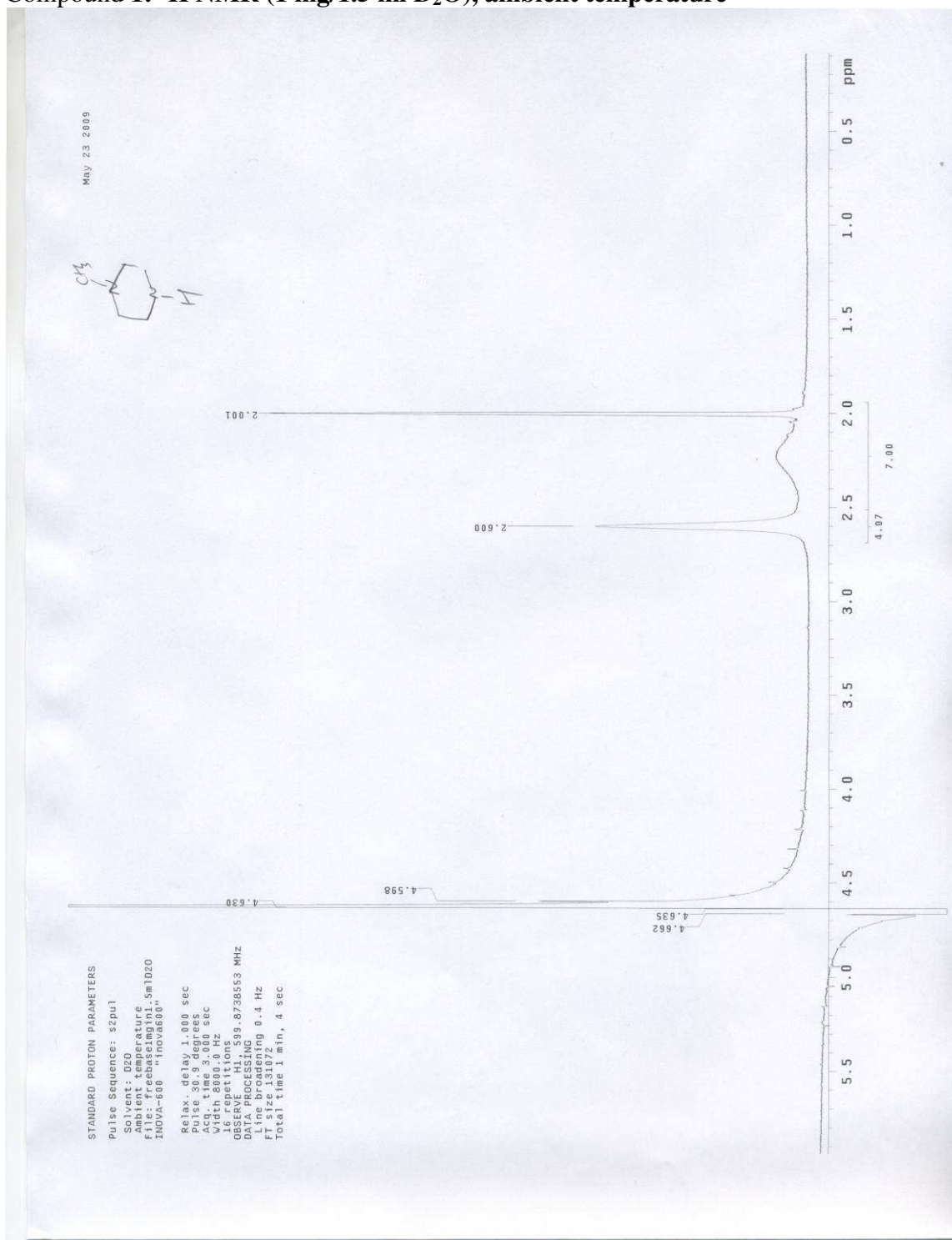


Fig. S4.

Compound 1:  $^1\text{H}$  NMR (75 mg/1.5 ml  $\text{D}_2\text{O}$ ), ambient temperature

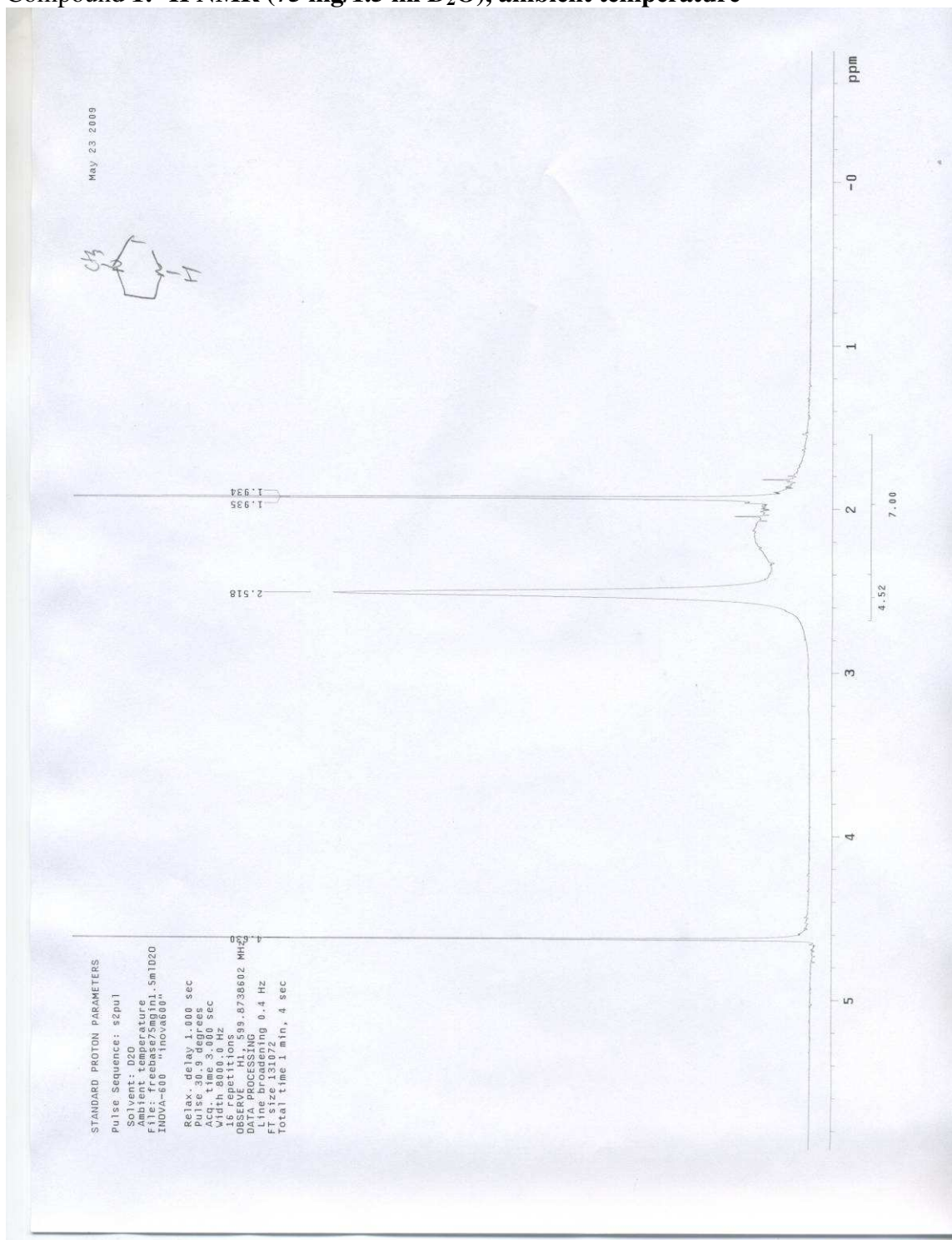


Fig. S5.

Compound 2a/b:  $^1\text{H}$  NMR (75 mg/1.5 ml  $\text{D}_2\text{O}$ ), ambient temperature

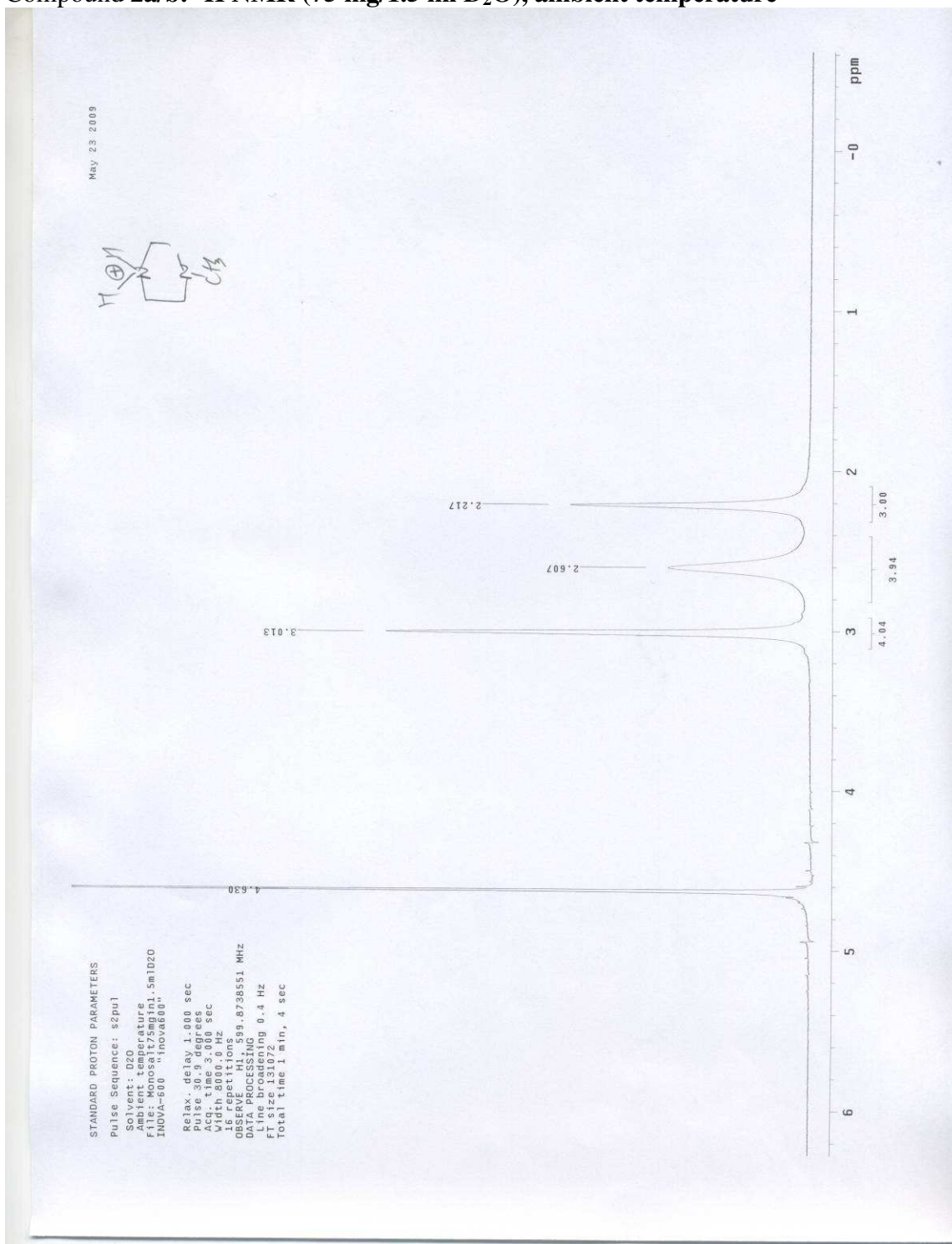


Fig. S6.





Compound 3:  $^1\text{H}$  NMR (75 mg/1.5 ml  $\text{D}_2\text{O}$ ), ambient temperature

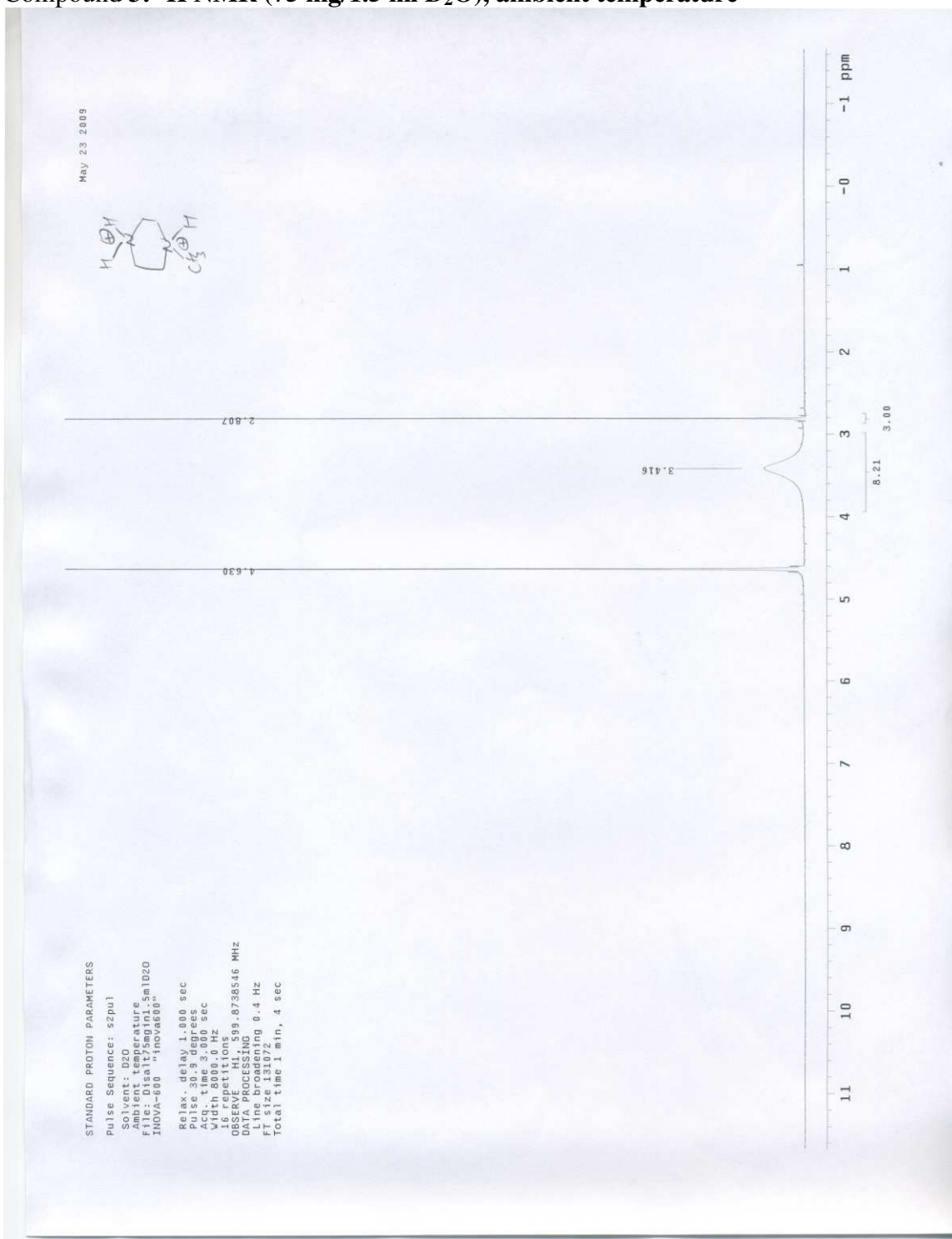


Fig. S8.

Compound 1:  $^1\text{H}$  NMR (75 mg/1.5 ml  $\text{CD}_2\text{Cl}_2$ ), ambient temperature

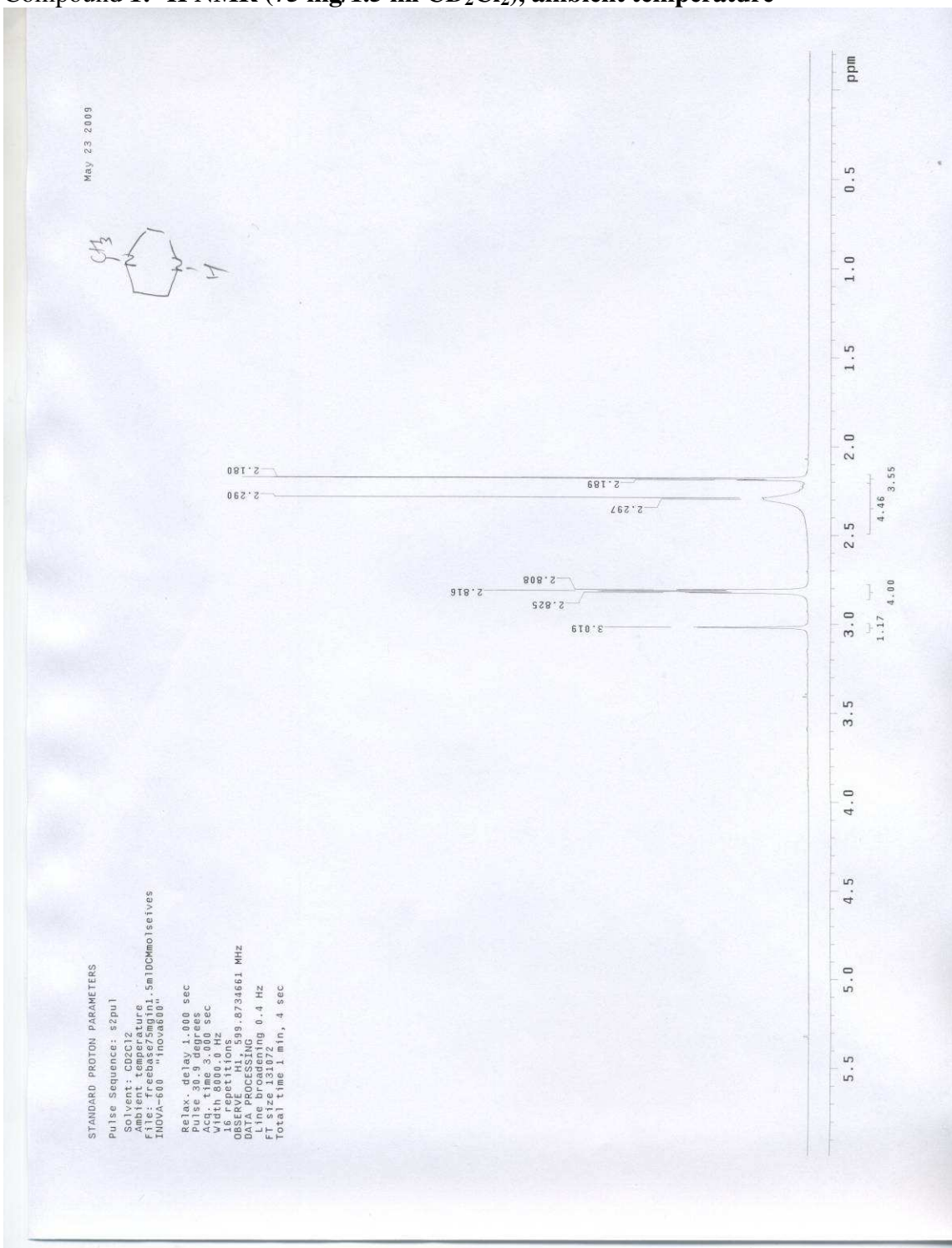


Fig. S9.

Compound 2a/b:  $^1\text{H}$  NMR (75 mg/1.5 ml  $\text{CD}_2\text{Cl}_2$ ), ambient temperature

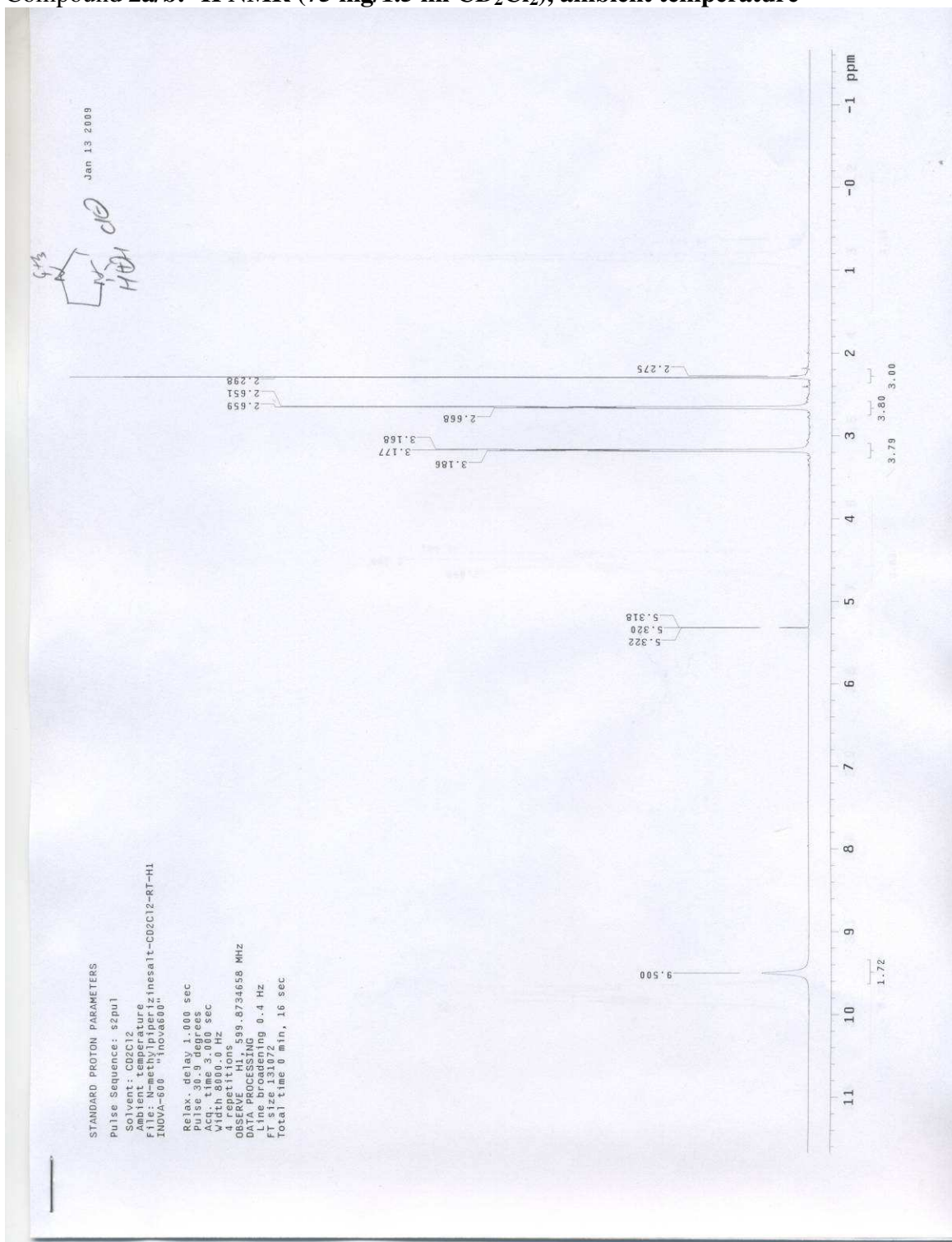


Fig. S10.



Compound 2a/b:  $^1\text{H}$  NMR (75 mg/1.5 ml  $\text{CD}_2\text{Cl}_2$ ), 166 K

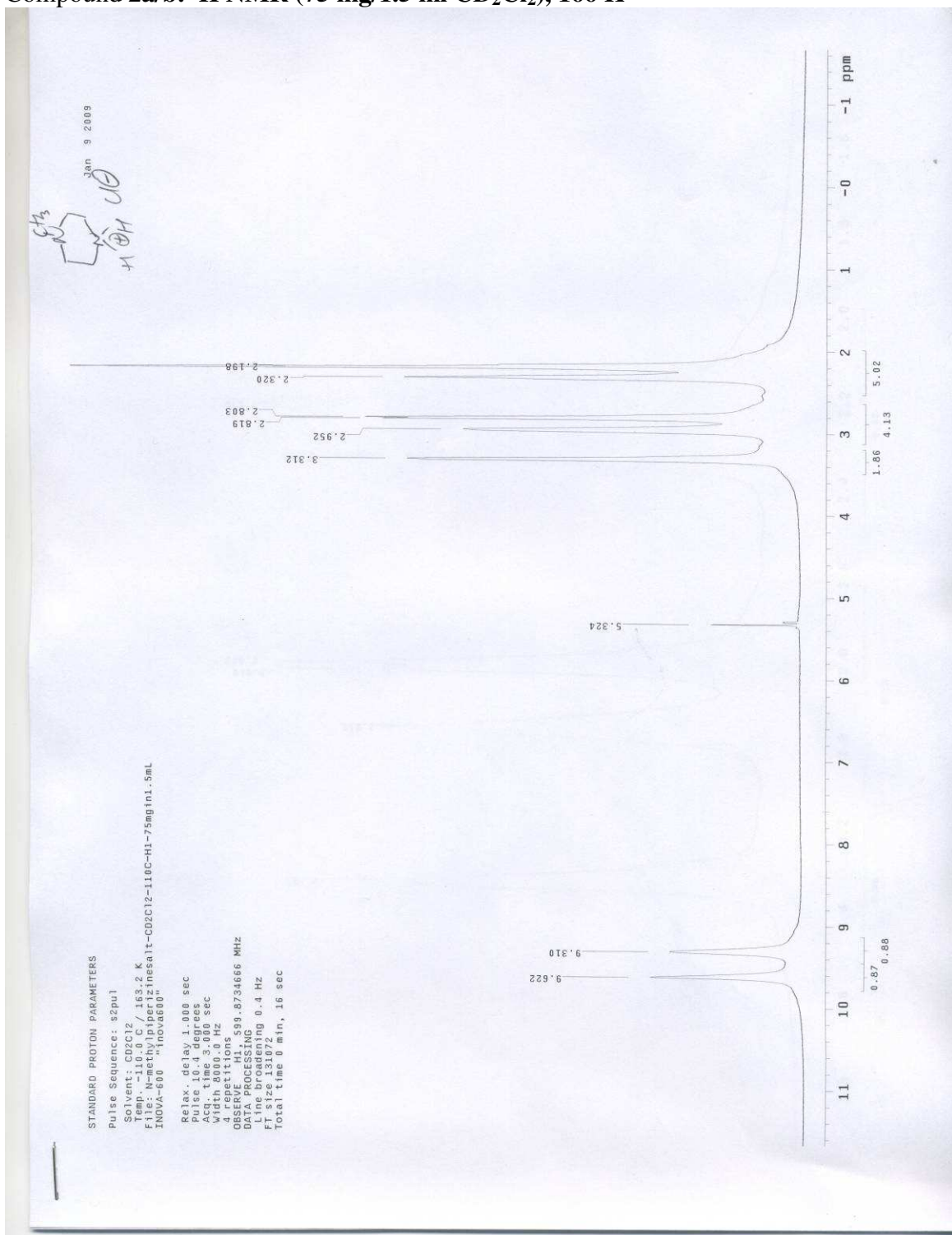


Fig. S11.

Compound 2a/b: COSY (75 mg/1.5 ml CD<sub>2</sub>Cl<sub>2</sub>), 166 K

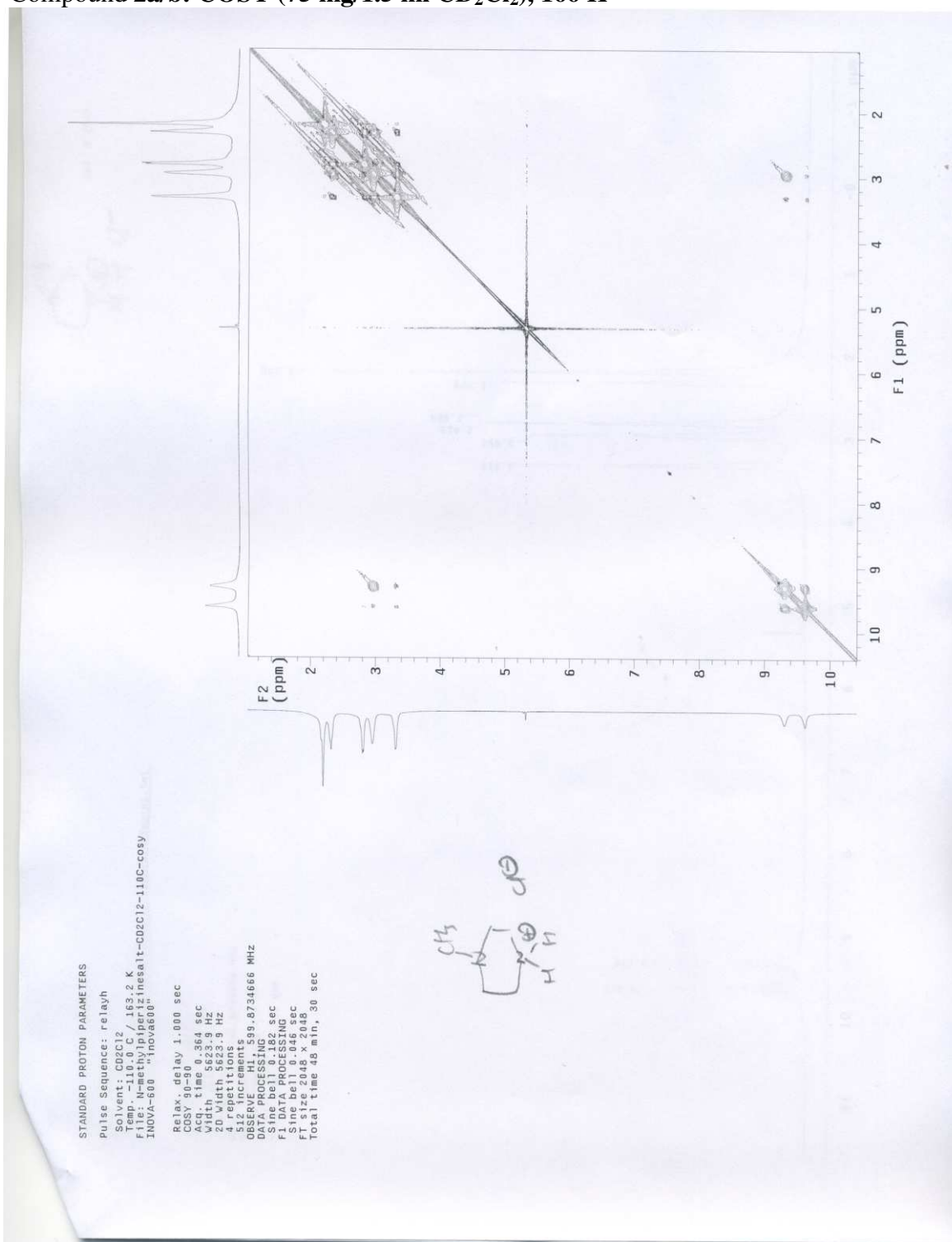
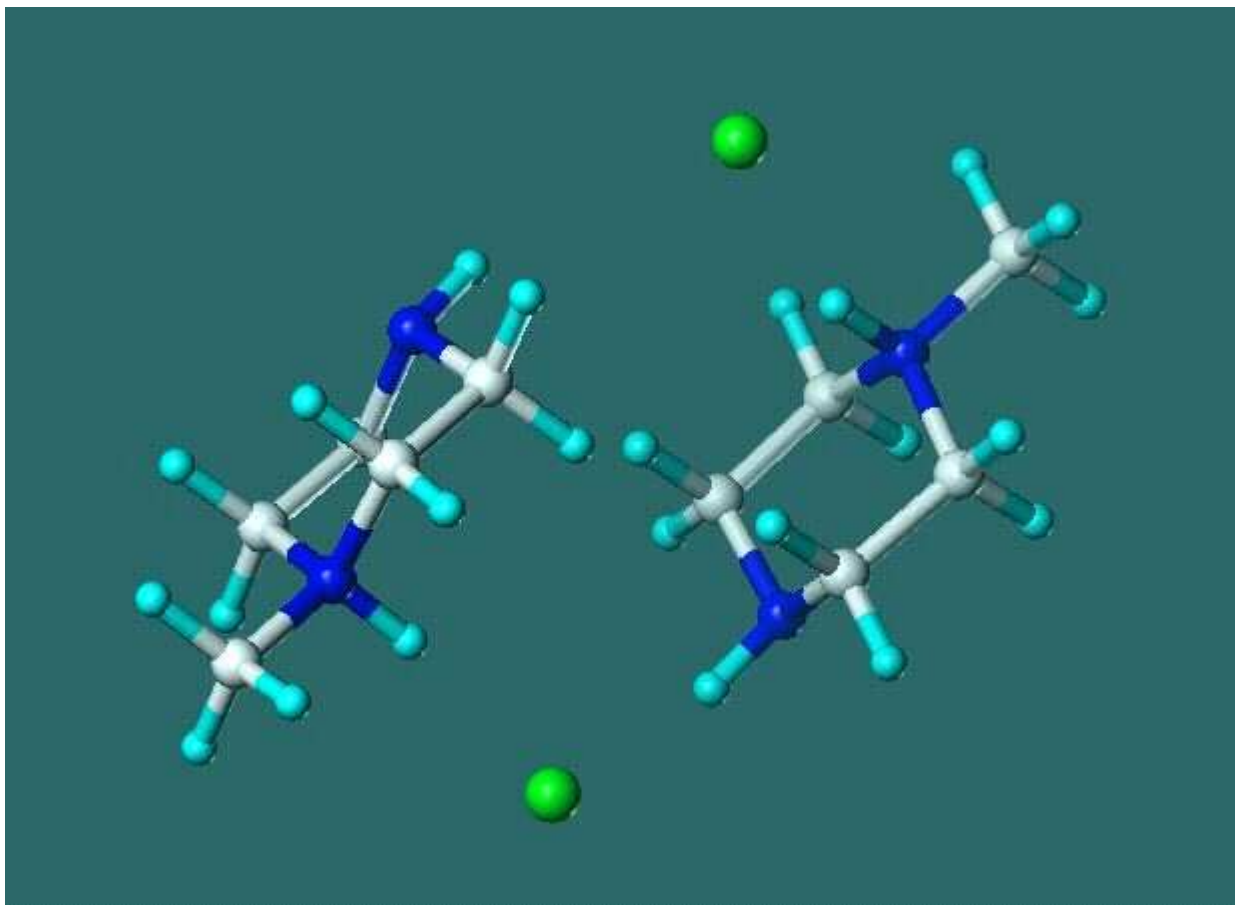
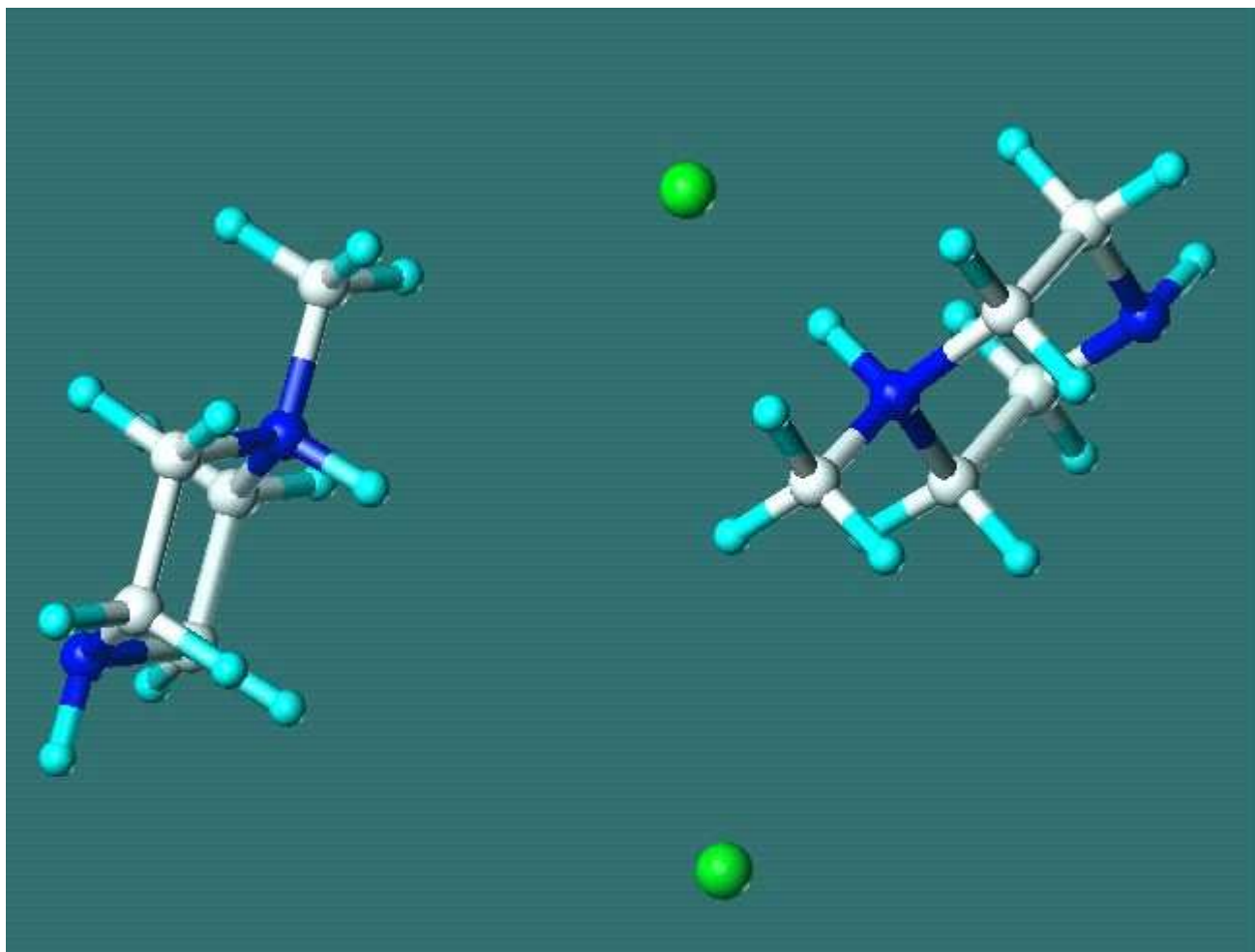


Fig. S12.



**Fig. S13.** The structure of the N-methyl-piperazine HCl dimer from the last configuration of the Monte Carlo simulation with CHELPG charges in dichloromethane. Protonation at the tertiary nitrogen. Distance of the ring centers is 5.2 Å. N(t)H..Cl hydrogen-bond distances are 2.19, 2.23 Å. N(s)H..Cl hydrogen-bond distances are 2.74, 2.96 Å.



**Fig. S14.** The structure of the N-methyl-piperazine HCl dimer from the last configuration of the Monte Carlo simulation with CHELPG charges in aqueous solution. Protonation at the tertiary nitrogen. Distance of the ring centers is 8.3 Å. N(t)H...Cl hydrogen-bond distance is 2.10 Å.

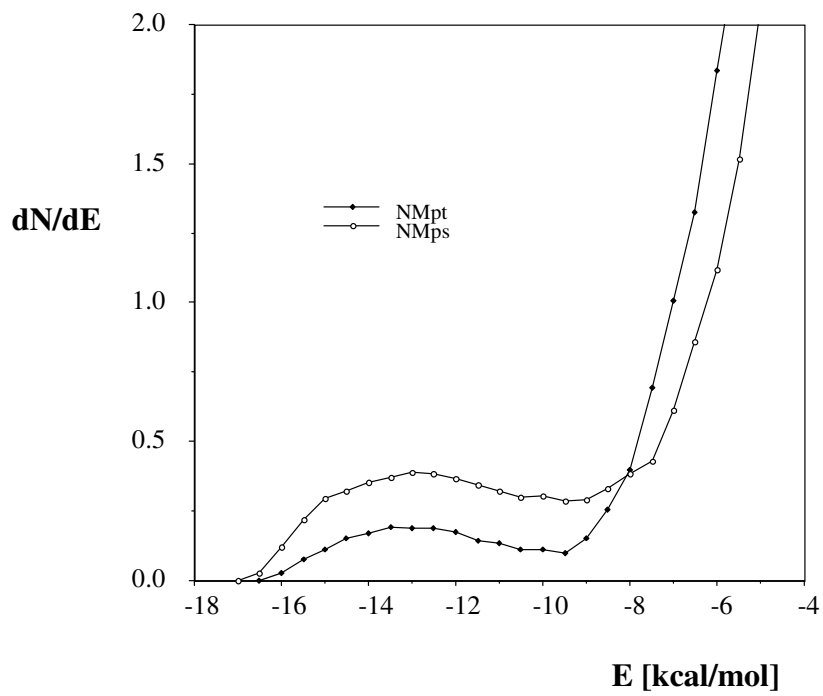


**Fig. S15.** Water- protonated N-methyl piperazine pair-energy distribution functions for NMpt and NMps solutes.

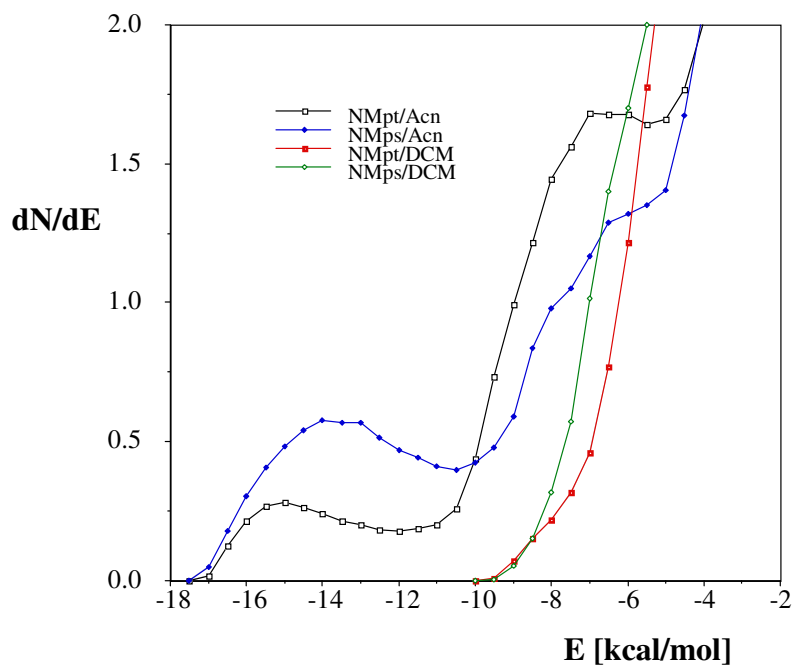


**Fig. S16.** Solute-solvent pair-energy distribution functions for NMpt and NMps solutes in acetonitrile and dichloromethane solvents.